Extended Abstracts of the 2013 International Conference on Solid State Devices and Materials, Fukuoka, 2013, pp666-667

First-Principles Simulations Applied to Graphene Nanoribbon Transistors

Mari Ohfuchi

Fujitsu Laboratories Ltd.
10-1 Morinosato-wakamiya, Atsugi, Kanagawa 243-0197, Japan
Phone: +81-46-250-8194 E-mail: mari.ohfuti@jp.fujitsu.com

We developed methods to introduce a gate electric field to first-principles electron transport calculations that do not require empirical parameters as a useful tool for investigating novel nanodevices. We can place any number of gates anywhere without increasing the computational cost through the analytical expression of the potential produced by a surface charge as a gate model. Equivalent circuit analysis transforms from the electron density of the surface charge ρ_G to the gate voltage V_G. Applying these methods to graphene nanoribbon (GNR) transistors, we demonstrated the allocability and multiplicity of gates and showed the dependence on channel length L_{Ch} of the transfer characteristics and the quantum capacitance of the channel C_Q for specific device structures.

1. Introduction

The non-equilibrium Green function (NEGF) method combined with first-principles calculations has been used to investigate the electron transport properties of various materials [1-3]. This arises from taking advantage of the density functional theory (DFT) where any empirical parameters dependent on the materials under study are not required. From an electronics point of view, it is desirable to investigate the transport properties with realistic geometries containing metal gate electrodes, as intensively investigated using a tight-binding approximation [4]. Only a few studies have been attempted using first-principles due to the high computational cost of this approach. In this work, we develop the methods that introduce a gate electric field to first-principles electron transport calculations without increasing the computational cost.

2. Methods

We use NEGF methods based on DFT [2]. The wave functions are expanded with the pseudoatomic orbital set that has been shown to give accurate results for transport calculations [3]. A surface charge as shown in Fig. 1(a) is introduced as a gate model. The analytical expression of the potential $p(x, y)$ produced by the surface charge is as follows:

$$\frac{4\pi\epsilon_V}{Q_G}p(x,z) = (x+a)\log\left\{(x+a)^2+z^2\right\} + 2z\tan^{-1}\frac{x+a}{z} - (x-a)\log\left\{(x-a)^2+z^2\right\} - 2z\tan^{-1}\frac{x-a}{z} - a\log\frac{a}{\sqrt{a^2+z^2}}, \quad (1)$$

where Q_G (= $-e\rho_G$, where ρ_G is the electron density) is the charge density of the surface charge and ε_V is the vacuum dielectric constant. An example of $p(x, y)$ is shown in Fig. 1(b). We can use the potential by cutting out the unit cell of transport calculations, so the size of first-principles calculations does not need to be enlarged and we can place any number of gates anywhere.

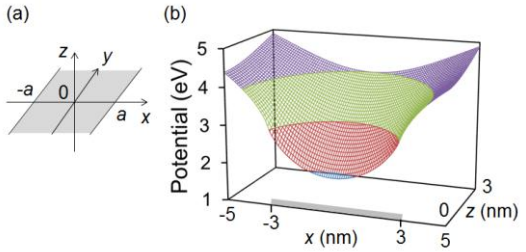

Fig. 1 (a) Schematic diagram of a surface charge as a gate model. (b) $p(x, y)$ produced by the surface charge, where a = 3 nm and $\rho_G = -10 \times 10^{12}$ cm^{-2}. The gray line schematically represents the position of the surface charge.

3. Graphene nanoribbon transistors

Allocability and multiplicity of gates

We examine four graphene nanoribbon (GNR) transistors with different gate geometries: D1, D2, D4, and S1. The symbols D and S represent double gates and a single gate, respectively, and the figures are the lengths between the gates and the channel L_G in nm. The schematic diagram for D1 is shown in Fig. 2(a). We use lithium (Li) doped GNRs as shown in Fig. 2(b) as leads, and the GNR without Li atoms as a channel with a length of 6.82 nm. All of the geometries can be studied using the same unit cell without increasing the computational cost.

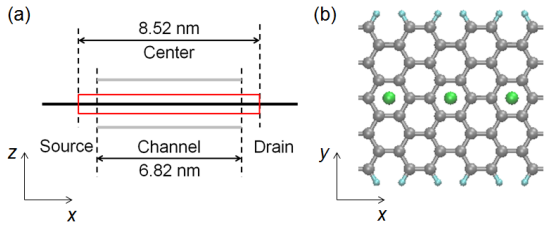

Fig. 2 (a) Schematic diagram of D1. The black line represents a GNR. The red rectangle denotes the unit cell in the center region. The gray lines indicate the positions of gate surface charges. (b) Model of GNRs. The gray, blue, and green spheres represent carbon (C), hydrogen (H), and lithium (Li) atoms, respectively. The C-C and H-C bond lengths are 0.142 and 0.108 nm, respectively. The distance between Li atoms and GNRs is 0.185 nm.

Performing electron transport calculations for ρ_G and a source-drain voltage V_{DS} as parameters, we obtain I_{DS}-ρ_G characteristics shown in Fig. 3(a). The current saturation is observed with high values of ρ_G. However ρ_G is difficult to

compare to experimental data. We attempt to transform from ρ_G to the gate voltage V_G, through the equivalent circuit as shown in Fig. 3(b).

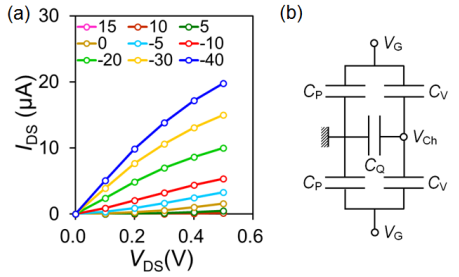

Fig. 3. (a) I_{DS}-V_{DS} characteristics for D1. The numerical values in the figure represent ρ_G (10^{12} cm^{-2}). (b) Equivalent circuit.

The electron density ρ_{Ch} and channel voltage V_{Ch} can be obtained from the result of the transport calculations. Fig. 4(a) shows the induced electron ρ in the center region, which is averaged to yield ρ_{Ch}. V_{Ch} can be read from the energy shift in the transmission, as seen in Fig. 4(b). ρ_{Ch} and V_{Ch} for four gate geometries are summarized in Fig. 5.

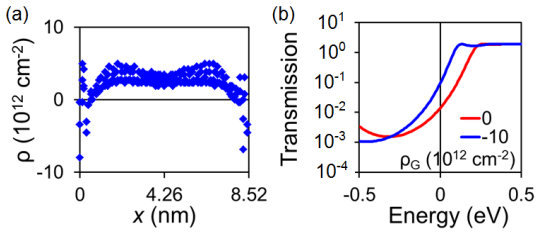

Fig. 4 Results of transport calculations of D1 for $\rho_G = -10 \times 10^{12}$ cm^{-2}. (a) Induced electron density of C atoms in the center region. (b) Transmission at $V_{DS} = 0$ with the result for $\rho_G = 0$.

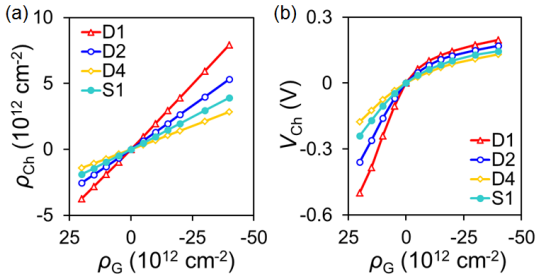

Fig. 5 (a) ρ_{Ch} and (b) V_{Ch} of four GNR transistors with different gate geometries.

The gate capacitance C_V is determined from the vacuum dielectric constant and thickness L_G – 0.085 nm (graphene charge distribution). Adding Q_{Ch}/C_V ($Q_{Ch} = e\rho_{Ch}$) to V_{ch} gives V_G. Finally we obtain the transfer characteristics shown in Fig. 6(a). The minimum current energy is shifted from zero. This arises from charge transfer to the channel from the leads where the GNRs are doped by Li atoms. We can see the longer L_G values and fewer gates lead to weaker gate effects, which is consistent with previous work with realistic geometries in a tight-binding scheme [4]. Fig. 6(b) shows the quantum capacitance of the channel ($C_Q = \Delta Q_{Ch}/\Delta V_{Ch}$). They are expectedly identical among all cases.

Channel length dependence

Fig. 7(a) shows I_{DS}-V_G characteristics for D1 with L_{Ch} =

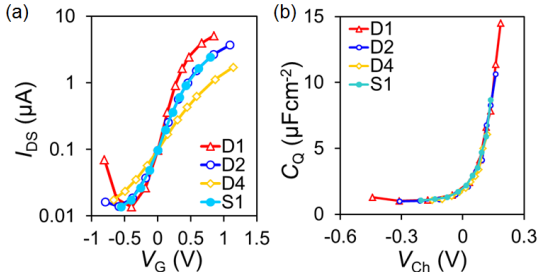

Fig. 6 (a) I_{DS}-V_G characteristics at $V_{DS} = 0.1$ V and (b) C_Q of four GNR transistors with different gate geometries.

6.82 and 13.6 nm at $V_{DS} = 0.1$ V. As expected from ballistic transport, the On current for both values of L_{Ch} are the identical. On the other hand, the Off current is reduced by a factor of 10^3 for the longer channel. This results due to lower tunneling between the leads in the energy gap for the longer L_{Ch} distance. The minimum current energy is shifted upward for the longer L_{Ch} value, indicating a narrower energy gap, which results from the doped GNR leads having a band gap around –1 eV. The subthreshold swing can be read to be 330 and 80 meV/dec for L_{Ch} = 6.82 and 13.6 nm, respectively, which is also consistent with the previous work [4].

We can clearly see the energy gaps in Fig. 7(b). The values of C_Q in their gaps are finite for both values of L_{Ch} and smaller for the longer channel. Isolated semiconducting GNRs have no states in the band gap, however GNRs connected to leads are considered to have a finite C_Q depending on the channel length and perhaps the contacts. Thus C_Q in a particular device structure can be determined.

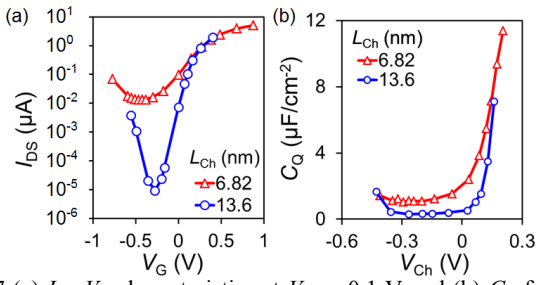

Fig. 7 (a) I_{DS}-V_G characteristics at $V_{DS} = 0.1$ V and (b) C_Q for D1 with L_{Ch} = 6.82 and 13.6 nm.

4. Summary

We developed the methods to introduce a gate electric field to first-principles electron transport calculations without increasing the computational cost. Using GNR transistors, we showed the allocability and multiplicity of gates and the dependence of the transistor properties on channel length. The quantum capacitance of the channel material for a particular device structure was also obtained. Our methods provide a useful tool to investigate novel nanodevices with various materials and architectures.

References

[1] T. Ozaki *et al.*, Phys. Rev. B **81** (2010) 035116.
[2] H. Jippo *et al.*, Phys. Rev. B **84** (2011) 075467.
[3] M. Ohfuchi *et al.*, Appl. Phys. Express **4** (2011) 095101.
[4] Y. Ouyang *et al.*, IEEE Trans. Electron Devices **54** (2007) 2223.